User Fairness in Energy Harvesting-Based LoRa Networks With Imperfect SF Orthogonality

Fatma Benkhelifa, *Member, IEEE*, Zhijin Qin, *Member, IEEE*, and Julie A. McCann, *Member, IEEE*

***Abstract*— Long range (LoRa) demonstrates high potential in supporting massive Internet-of-Things (IoT) applications. In this paper, we study the resource allocation in energy harvesting (EH)-enabled LoRa networks with imperfect spreading factor (SF) orthogonality. We maximize the user fairness in terms of the minimum time-averaged throughput while jointly optimizing the SF assignment, the EH time duration, and the transmit power of all LoRa users. First, we provide a general expression of the packet collision time between LoRa users which depends on the SFs and EH duration requirements of each user. Then, we develop two SF allocation schemes that either assure fairness or not for the LoRa users. Within this, we optimize the EH time and the power allocation for single and multiple uplink transmission attempts. For the single uplink transmission attempt, the optimal power allocation is obtained using bisection method. For the multiple uplink transmission attempts, the suboptimal power allocation is derived using concave-convex procedure (CCCP). Our results unearth new findings. Firstly, we demonstrate that the unfair SF allocation algorithm outperforms the others in terms of the minimum data rate. Additionally, we observe that co-SF interference is the main limitation in the throughput performance, and not really energy scarcity.**

***Index Terms*— LPWANs, Long Range (LoRa) networks, energy harvesting, max-min fairness, spreading factors, concave-convex procedure.**

I. Introduction

INTERNET of Things (IoT), sensor networks, and cyber-physical systems have gained extensive interest as they are used in a wide range of applications to enable their automation, resource optimization, resilience to change and failure, and sustainability. Applications include smart cities, smart farming/agriculture, health care, public safety, etc., [2]. Many such systems involve the use of massive numbers of deployed devices with limited resources which need to deliver reliable data to potentially critical applications.

Manuscript received August 13, 2020; revised January 14, 2021; accepted March 15, 2021. Date of publication March 23, 2021; date of current version July 15, 2021. This work is partially supported by the EPSRC Grant "Science of Sensor Systems (S4)" Programme (EP/N007565/1), the Alan Turing Institute and the Lloyd's Register Foundation. This work was presented in part at the IEEE International Conference on Communications (ICC'2019), Shanghai, China. The associate editor coordinating the review of this article and approving it for publication was L. Wei. *(Corresponding author: Fatma Benkhelifa.)*

Fatma Benkhelifa and Julie A. McCann are with the Computing Department, Imperial College London, London SW7 2AZ, U.K. (e-mail: f.benkhelifa@imperial.ac.uk; j.mccann@imperial.ac.uk).

Zhijin Qin is with the School of Electronic Engineering and Computer Science, Queen Mary University of London, London E1 4NS, U.K. (e-mail: z.qin@qmul.ac.uk).

Color versions of one or more figures in this article are available at https://doi.org/10.1109/TCOMM.2021.3068304.

Digital Object Identifier 10.1109/TCOMM.2021.3068304

Many of these systems span multikilometres, such as smart water networks and precision farms which have motivated the development of communication technologies that support low power operation. To achieve this, they operate at relatively low data rates. Low power wide area networks (LPWANs) are gaining considerable interest across the world with countries such as the Netherlands deploying a LPWAN country-wide [3]. Many standard technologies are competing to model LPWAN, such as SigFox [4], Weightless, Narrowband IoT (NB-IoT) [5] and Long Range (LoRa) [6].

Among the existing standards for LPWAN, LoRa has captured great attention from both academia and industry by its strength lying on the ability to cover large geographical distances and on the adopted chirp spread spectrum (CSS) modulation that assigns different spreading factors (SFs) to users to make it resilient to external interference [6]. LoRa wide-area network (LoRaWAN) operates in the sub-GHz frequency bands [6]. In Europe, LoRaWAN uses the EU industrial, scientific, and medical (ISM) 868 MHz frequency. For this band, there are eight channels: six with SF from 7 to 12 with bandwidth 125 kHz and one with SF 7 with bandwidth 250 kHz, and one with Gaussian frequency-shift keying (GFSK) at 50 kbps data rate. In addition, the European frequency regulations impose duty cycle restrictions for the 868 MHz sub-bands, either 1% or 10% [7]. For the medium access control (MAC) layer, the end user devices access the channel using the pure ALOHA for transmitting their packets. For the network architecture, LoRaWAN employs a star-of-stars topology where gateways relay the data transmissions between the end user devices and the server.

A. Related Works

So far, most research in LoRa networks has focused on the studies of scalability, coverage, and reliability considering the co-SF and/or inter-SF interference. In [8], the uplink coverage probability of a single LoRa gateway was derived using stochastic geometry and two-link outage conditions were solved showing that the scalability of LoRa is related to co-SF interference. In [9], the Poisson cluster processing was adopted to model the distribution of LoRa users and the coverage probability was derived by considering the interference from LoRa users as well as non-LoRa users. In [10], the average system packet success probability (PSP) was analyzed using stochastic geometry for a LoRa system using the unslotted ALOHA random access protocol. Also, an adaptive SF allocation

algorithm was proposed which maximizes the average system PSP. In [11], the resource allocation of uplink transmissions in LoRa networks was investigated where the minimum data rate of LoRa users was optimized through the joint optimization of the channel assignment and the power allocation using a many-to-one matching game. For each channel assigned, the optimal power allocation was obtained. In [12], a theoretical analysis of the achievable LoRa throughput was analyzed taking into consideration the co-SF interference between users using the same SF as well as the inter-SF interference between users using different SFs. In [13], the scalability of a LoRa network was analyzed in the presence of imperfect orthogonality between SFs. The coverage probability was evaluated by modelling interference as Poisson point processes under duty cycled ALOHA. In [14], the minimum throughput rate was maximized for NOMA-enabled LPWAN while optimizing the channel allocation, the transmission time allocation, and the power allocation. Only one transmission attempt was considered per node independently of the SF value.

Additionally, LoRa networks are know for capture effect which means that concurrent transmissions are possible if their power difference is above a certain value. Also, it means that only the node with the highest power will survive its transmission among the other concurrent transmissions. Some papers considered the capture effect in their analysis namely [8], [10], [15]. In [8], the authors defined the capture effect as the ratio between the received power of the desired user over the maximum received power from the interferer being above 6 dB. In [10], the authors defined the capture effect as the ratio between the received power of the desired user and the sum of received power of all interferers being above a certain threshold. Their capture effect definition is very similar to the signal to interference ratio (SIR). The SIR thresholds are commonly named co-subchannel rejection thresholds and their values are different from the well-known 6 dB value. In [15], the authors defined the capture effect as the average of the conditional probability of having SIR above a certain threshold over the number of interferers. The number of interferes can be from 1 to ∞. Within this context, our work can be seen as a generalization of the capture effect where all nodes can transmit independently of the power difference between the desired user and the interferer. Every node can transmit as long as they are satisfying the SF constraint, duty cycle restrictions, and the energy constraints.

Nevertheless, spreading factor allocation is quite rudimentary. In [16], a packet error rate fairness is efficiently optimized by controlling the power and the spreading factor while avoiding the near-far problems. In [17], a fair adaptive data rate allocation was proposed to achieve a fair collision probability based on [16] among all used data rates and a transmission power control algorithm was developed to exhibit data rate fairness among the users. In [18], the two algorithms EXPLoRa-SF and EXPLoRa-AT were proposed to allocate the SFs that outperform LoRa's basic Adaptive Rate Strategy (ADR). EXPLoRa-SF tries to equally divide the SFs between the users while respecting the received signal strength (RSSI) values and relevant constraints. EXPLoRa-AT is more complex algorithm than EXPLoRa-SF and tries to fairly allocate the air time between users. In [13], three SF allocation schemes were analyzed which show that equal interval-based scheme outperforms the equal-area-based scheme and path-loss-based scheme. In [19], improving user fairness and reducing energy consumption were considered by jointly allocating power and SF with imperfect orthogonality. The many-to-one matching algorithm was considered for the SF assignment. The power allocation was obtained using two types of constraint transformations: linearized and quadratic. In [20], a linear integer program was developed to optimize the SF allocation while considering capture effect and imperfect SF orthogonality with guaranteeing on the target success probability. In [21], an SF allocation algorithm was proposed based on K-means clustering and outage probabilities were evaluated without considering retransmissions for large-scale LoRa networks. In [22], an adaptive SF allocation was proposed which enabled every device supporting single data rate to achieve multi-data rates. The scheme was implemented on real LoRa devices and throughput improvement was proven.

LoRa resilience is limited because the devices are powered by finite energy (battery-based) sources. The battery replacement cost and maintenance are high. It is estimated that the global battery market size for IoT will reach USD 15.9 billion in 2025 [23]. Additionally, being battery-powered limits where such devices can be deployed. The cost of battery replacement is even higher for devices positioned in extreme environments that are difficult or even dangerous to access. Thus, energy efficiency is a major challenge in LoRa networks and has been addressed in various studies [24], [25] in order to extend the battery lifetime of sensor devices. However, improving energy efficiency is not sufficient in itself. On the other hand, energy harvesting (EH) is one way to ensure sustainable operation or at least elongated life-times. EH can be harvested from different types of sources, such as solar, wind, electromagnetic, radio frequency (RF) [26]. The latter technique can be obtained from dedicated transmitters (that exist specifically to provide energy) or ambient energy (transmitters that exist in the environment already e.g. WiFi). However, research on EH-enabled LoRa networks is still at its infancy. In [27], a battery-less LoRa wireless sensor was designed for road condition monitoring and is powered by the vibrations harvested by an electromagnetic energy harvester based on a Halbach configuration. In [28], a novel floating device was proposed with a multi-source energy harvesting technique, which harvests solar and thermoelectric energy. The work was extended in [29], to reduce the power consumption in the listening phase. These works do not carry out energy budgeting or optimization to provide energy neutral guarantees.[1]

B. Motivation and Contributions

In this paper, we study the resource allocation in LoRa networks by maximizing the minimum time-averaged data rate of the LoRa users during a time window T. The LoRa users

[1]Energy neutral operation (ENO) is a method for managing the energy utility of energy harvesting nodes [30]. It is an operation mode that defines a balance between the consumed energy, the harvested energy and the stored energy.

are self-powered and harvest energy from an external source to perform uplink transmissions. The harvested energy can be of any type such as solar and RF. The remaining energy is stored in the battery and each LoRa user might transmit once or many times during T. First, we propose two types of algorithms that allocate the SFs either fairly or unfairly between the users. The unfair SF allocation scheme allocates the different SFs to active LoRa nodes equally; and hence the LoRa nodes with higher SFs occupy the channel for longer time than the LoRa nodes assigned to lower SFs. The fair SF allocation scheme allocates the users in a way that the LoRa nodes occupy the channel for equal average times independently of their SFs. We compare the proposed algorithms to other related algorithms in the literature. We optimize the EH time using a one-dimensional search method. For the single attempt uplink transmission, we obtain the optimal power allocation between LoRa users. For multiple attempts, we optimize the power allocation using the concave-convex procedure (CCCP), which uses a first-order Taylor approximation to derive a concave bound on the nonconcave objective function. In the simulation results, we harvest the energy from ambient RF signals and we compare our proposed solution to different baseline schemes. To the best of our knowledge, this paper is the first to address the resource allocation in LoRa networks while maximizing the minimum time-averaged data rate using the EH capabilities to power its uplink transmissions. The EH source can be of any type as long as it is independent of the LoRa frequency band. The contributions of this paper are summarized as follows:

- We explicitly express the packet collision time between users using the same SF and different SFs, and we show that its expression depends on the EH time and SFs.
- We propose a general framework that considers the interference between users transmitting at the same time over nonorthogonal waveforms. Thus, the multiuser interference between the users occurs either due to colliding users in the time or due to nonorthogonality between spreading coded waveforms.
- For one attempt of uplink transmissions, we observe that the inter-SF interference (if considered) is neutralized thanks to use of the expression of the packet collision time for a specific value of the EH time.
- For both single and multiple transmission attempts, we observe that the unfair SF allocation outperforms all the other SF allocation approaches in terms of the minimum rate of LoRa users.
- Moreover, we show that co-SF interference is the main limitation of the system performance, and not really the energy scarcity.

C. Structure of the Paper

The remainder of this paper is organized as follows. The system model is presented in Section II. The proposed packet collision time between LoRa users is presented in Section III. The formulated max-min throughput optimization problem and solutions are presented in Section IV. The numerical results are presented in Section V. Section VI concludes the paper.

II. System Model

In this section, we consider the uplink transmissions in a LoRa network during the time window T powered by ambient energy.[2] Since LoRaWAN employs a star-of-stars topology, we consider one gateway that relays the data transmissions between U LoRa end users and the server. The U LoRa users are uniformly distributed in a circle of radius R centred around the gateway. Each LoRa user is self-powered by harvesting energy from external sources and stores the remaining energy in a rechargeable battery with limited capacity. The external sources of energy can be of any type (solar or RF or others), and only one condition applies if RF source is considered, a frequency band different from LoRa band (868 MHz) is used. This condition is considered to alleviate the possibility that the energy harvesting signals cause additional interference to LoRa gateway.

The considered time window T is divided into K time slots[3] of equal duration, as illustrated in Fig. 1. During each time slot, each LoRa user is either transmitting data or harvesting energy depending on its SF assigned by the gateway. In addition, the number of uplink transmission attempts can be one or many, which is the choice of the LoRa users and is limited by the SF assigned by the gateway which is explained in what follows.

At the time slot $k = 1, \ldots, K$, the channel between the n-th LoRa user and the gateway is modelled as a Rayleigh fading channel with path loss as

$$g_n(k) = h_n(k) \left(d_n(k)\right)^{-\alpha}, \tag{1}$$

where $n = 1, \ldots, U$, $h_n(k)$ is the small scale fading that is exponentially distributed with unit mean, $d_n(k)$ is the distance between the n-th LoRa user and the gateway, at the k-th time slot, and α is the path loss exponent.

A. Physical Layer of LoRa

For the LoRa physical layer, the bandwidth BW is equal to 125 kHz or 250 kHz. For $BW = 125$ kHz, we have 8 channels and maximum 6 SFs per channel. We assume that each LoRa user has always access to one free channel.[4] The n-th LoRa user is assigned to an SF as

$$SF_n \in \mathcal{S} = \{7, \ldots, 12\}. \tag{2}$$

We assume that the assignment of SF_n to the n-th user is independent of the time slot k and remains the same during the

[2]The use of time window T is because of the LoRa physical layer precisely the CSS modulation. It allows all users to transmit more than once independently of their SF. Also, it allows to have a fair comparison between users transmitting during different duration. If we remove the time window T, all users will be transmitting once during their corresponding transmission time-on-air depending on their assigned SF.

[3]The notation of time slots is used only for modeling purposes. LoRa uses unslotted ALOHA protocol and this setting is still in accordance with this protocol. The notation of time slots is used to represent the time during which each user can perform up to one single transmission attempt and to keep track of the number of transmission attempts. The start time of a packet transmission is random and is not restricted to the start of the time slot.

[4]The channel access selection is out of the scope of this work and might be considered in future works.

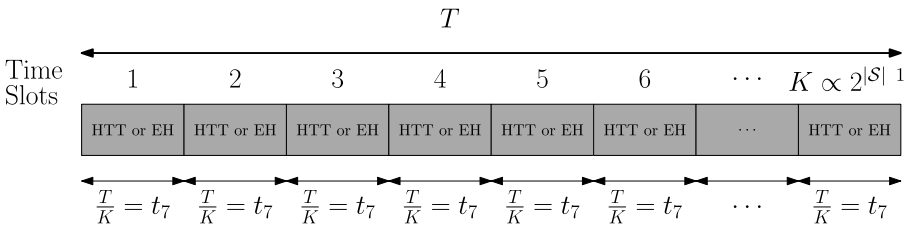

Fig. 1. Time window T with K time slots of duration t_7.

whole time window T. The corresponding time-on-air (ToA) is given by

$$T_{a,n} = Nb_n \, T_{s,n} = Nb_n \, \frac{2^{SF_n}}{\text{BW}}, \tag{3}$$

where Nb_n is the number of symbols transmitted by the nth user, $T_{s,n}$ is the corresponding symbol duration, and the bandwidth BW is most likely equal to 125 kHz for most LoRa channels.

In addition, the European frequency regulations impose duty cycle restrictions for the 868 MHz frequency band, either 1% or 10% [7]. This means that each LoRa user should stay silent $(1-d)\%$ of the packet duration once the transmission happens over one channel, where d is the duty cycle generally equal to 1% or 10%. Subsequently, the time-off per channel $T_{off,n}$ and the packet duration T_n of the n-th user are expressed as

$$T_{off,n} = \frac{1-d}{d} T_{a,n}, \quad \text{and} \quad T_n = \frac{T_{a,n}}{d}, \tag{4}$$

where $T_{a,n}$, $T_{off,n}$ and T_n belong to the spaces $\mathcal{T}_a = \{t_{a,i} = Nb_i \frac{2^i}{\text{BW}}, i = 7, \ldots, 12\}$, $\mathcal{T}_{off} = \{t_{off,i} = \frac{1-d}{d} Nb_i \frac{2^i}{\text{BW}}, i = 7, \ldots, 12\}$, $\mathcal{T} = \{t_i = \frac{Nb_i}{d} \frac{2^i}{d\text{BW}}, i = 7, \ldots, 12\}$, respectively. The symbols $t_{a,i}$, $t_{off,i}$ and t_i stand for the possible values of $T_{a,n}$, $T_{off,n}$ and T_n in the $\mathcal{T}_a$, $\mathcal{T}_{off}$, and $\mathcal{T}$, respectively. These spaces are all of the same dimension as the cardinality of $\mathcal{S}$, i.e. $|\mathcal{S}| = 6$.

In the following, we state a couple of properties satisfied by the LoRa users.

Property 1: For the n-th LoRa user, $T_{a,n}$ and $T_{off,n}$ are both proportional to SF_n. Increasing the SF increases both the time on air and the off time.

Property 2: If the number of symbols Nb_n is the same for all users, then we have $t_{a,i} = 2\ t_{a,i-1}, \forall i = 8, \ldots, 12$, and subsequently, $T_{a,n}$ becomes in the space

$$T_{a,n} \in \tilde{\mathcal{T}}_a = \{2^i t_{a,7}, i = 0, \ldots, 5\}. \tag{5}$$

Same property applies to $T_{off,n}$ and T_n.

Property 3: If $Nb_i < Nb_7$, $\forall i = 8, \ldots, 12$, then we satisfy the condition

$$t_7 > t_{a,i}, \quad \forall i = 7, \ldots, 12, \quad \textit{if } d = 1\%, \tag{6}$$

$$t_7 > t_{a,i}, \quad \forall i \leq 10, \quad \textit{if } d = 10\%. \tag{7}$$

The inequality $t_7 > t_{a,i}$ means that the user with the least $SF = 7$ (the lowest packet duration t_7) will not start transmitting again until the user with a higher $SF = i$ (a higher time-on-air duration t_i) has also finished transmitting.

Property 4: If the duty cycle is $d = 1\%$ and $Nb_i < Nb_7$, then Property 3 is satisfied and hence the condition $\sum_{i=7}^{12} t_{a,i} < t_7$ is satisfied.

This inequality $\sum_{i=7}^{12} t_{a,i} < t_7$ means that within a time slot of length t_7 all users are able to transmit once and no more than once. Also, it means if users are scheduled during orthogonal times, it is possible to do so within a total duration t_7.

In the sequel, we assume that most likely the duty cycle is equal to 1%. For simplicity, we assume that all users have the same number of symbols $Nb_i, \forall i$. Then, all properties 1-4 are satisfied. Precisely, we have $t_i = 2\ t_{i-1}$ (Property 2), $t_7 > t_{a,i}$, $\forall i$ (Property 3) and $\sum_{i=7}^{12} t_{a,i} = (2^6 - 1) t_{a,7} < t_7 = \frac{t_{a,7}}{d}$ (Property 4). In addition, the time slots are of duration t_7 and the number of time slots K is a multiple of $2^{|\mathcal{S}|-1}$.

B. Harvest-Then-Transmit (HTT) Protocol

The LoRa users are self-powered using the "harvest-then-transmit" (HTT) protocol where each LoRa user harvests first what it needs and then transmits its data. As shown in Fig. 1, within a certain time slot, the n-th LoRa user can be either in HTT mode or in EH mode. The selection of the HTT mode or the EH mode is depending on SF_n of the n-th LoRa user. For the EH mode, the user can harvest energy up to the time slot duration t_7. For the HTT mode, the user can harvest energy during a maximum duration equal to $(t_7 - T_{a,n})$ and then transmits its data to the gateway during its time-on-air $T_{a,n}$.

Actually, if the n-th LoRa user is assigned to SF_n, it can be in HTT mode at time slot k multiple of 2^{SF_n-7}, i.e. $\mod \left(k, 2^{SF_n-7}\right) = 0$, such that

$$k = m\ 2^{SF_n-7}, \quad \text{where } m = 1, \ldots, \left\lfloor \frac{K}{2^{SF_n} - 7} \right\rfloor. \tag{8}$$

Otherwise, the n-th LoRa users is in EH mode at time slot k not multiple of 2^{SF_n-7}, i.e. $\mod \left(k, 2^{SF_n-7}\right) \neq 0$. The number of EH time slots are due to the duty cycle restrictions which impose that a transmission attempt during $T_{a,n}$ should be accompanied with an off-time duration $T_{off,n}$. Here, we assume that the LoRa users are in the EH mode during the off-time duration. Fig. 2 presents the EH and HTT models under different SFs.

Let $\rho_n(k)$ be a binary variable indicating if the n-th user is transmitting or not, i.e. 1 for transmitting and 0 for not. The user is transmitting if it is in HTT mode and has a packet to transmit. Let $\rho_{1,n}(k)$ be a binary variable indicating if the

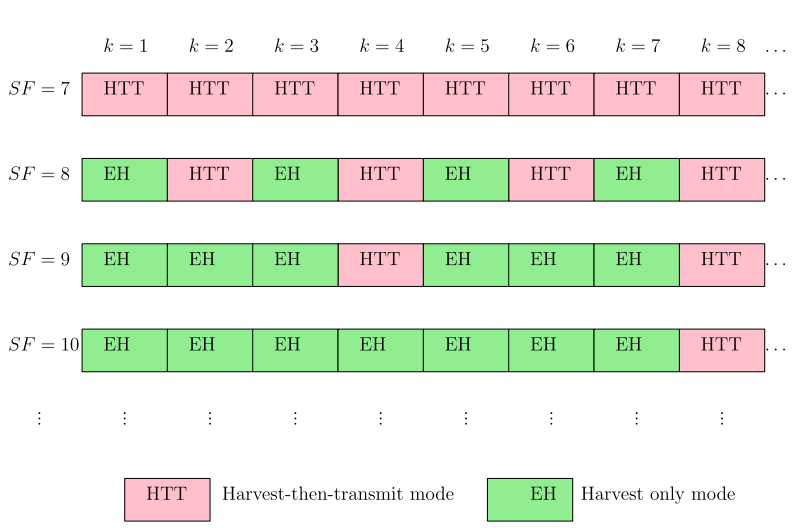

(a) EH and HTT modes depending on SFs.

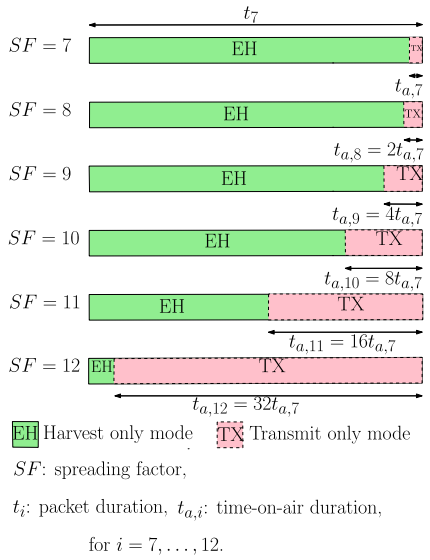

(b) HTT mode depending on spreading factors.

Fig. 2. Illustration of maximum number of transmission attempts $a_{n,max}$ and EH modes per SF during T with K time slots of width t_7.

n-th user is in HTT mode or EH only mode as

$$\rho_{1,n}(k) = \begin{cases} 1, & \text{if HTT mode i.e.} \mod \left(k, 2^{SF_n-7}\right) = 0, \\ 0, & \text{if EH mode i.e.} \mod \left(k, 2^{SF_n-7}\right) \neq 0. \end{cases} \tag{9}$$

In addition, we consider another binary variable $\rho_{2,n}(k)$ that defines if the user has a packet to transmit or not at the current time slot k in the HTT mode. So, a transmission attempt is defined by $\rho_n(k) = \rho_{1,n}(k)\rho_{2,n}(k) = 1$.

Let us denote $a_n(k)$ the number of transmission attempts at the n-th user in HTT mode at time slot k. $a_n(k)$ can be defined as $a_n(k) = \sum_{j=1}^{k} \rho_n(k)$, which happens at the time slot $\rho_n(k)k \propto 2^{SF_n-7}$, and is at least equal to one and upper bounded by the maximum number of transmission attempts that can happen during the total K time slots. The maximum number of transmission attempts for the n-th LoRa user is the maximum number of time slots in HTT mode that depends on SF_n and can be given by

$$a_{n,max} = \sum_{k=1}^{K} \rho_{1,n}(k) \leq \left\lfloor \frac{K}{2^{SF_n-7}} \right\rfloor. \tag{10}$$

C. Energy Harvesting at LoRa Users

Each LoRa user is harvesting energy from an external source of energy. The external energy harvesting source could be of any type, under the condition that it is not interfering with the band frequency of the LoRa users. For example, if it is from RF energy harvesting, we assume that the energy is harvested from a band frequency other than the 868 MHz. We assume that the harvested energy per time unit is known and uncontrollable. Let $E_n(k)$ be the harvested energy per time unit of the n-th user. Let $\tau_{e,n}(k)$ be the EH duration during the k-th time slot. For the n-th user, the harvested energy during a harvesting time $\tau_{e,n}(k)$ during the k-th time slot is given by

$$E_{h,n}(k) = \tau_{e,n}(k)E_n(k). \tag{11}$$

Since the LoRa user is the one that decides when to transmit, we can consider that each user can harvest energy during a total time less or equal to $(1-d)\%$ of the packet duration before performing a single transmission attempt. This adds a constraint on the harvesting time at k-th time slot

$$0 \leq \tau_{e,n}(k) \leq \tau_{e,n}^{max}(k) = t_7 - \rho_n(k)T_{a,n}, \tag{12}$$

where $\tau_{e,n,max}(k)$ is equal to $t_7 - T_{a,n}$ in HTT mode and t_7 in EH mode. Hence, the harvested power during each time slot k at the n-th user is given by

$$P_{h,n}(k) = \frac{E_{h,n}(k)}{T_{a,n}} = \frac{\tau_{e,n}(k)E_n(k)}{T_{a,n}}. \tag{13}$$

Remark 1: For each transmission attempt a_n, the n-th LoRa user can be in EH mode during a maximum number of time slots equal to $(2^{SF_n-7}-1)$ time slots of duration t_7 and then moves to the HTT mode during one time slot. Hence, it can be verified that, before each transmission attempt, the maximum total EH time duration is $(2^{SF_n-7}-1)t_7 + t_7 - T_{a,n}$, which is exactly equal to the off-time duration $T_{off,n} = \frac{1-d}{d}T_{a,n}$. Recall that $T_{a,n} = 2^{SF_n-7}t_{a,7}$. Then, the total EH time per one transmission attempt of the n-th user is constrained to $T_{off,n} = \frac{1-d}{d}T_{a,n}$.

Then, the available power budget that a certain user n can use to transmit during a certain time slot k is the cumulative sum of the harvested power minus the transmission power during the previous time slots. Other power consumption is assumed to be negligible for the moment. The available power can be expressed as

$$P_{A,n}(k) = \sum_{j=1}^{k} P_{h,n}(j) - \sum_{j=1}^{k-1} \rho_n(j)p_n(j). \tag{14}$$

Note that only at time slots k and j, user n is transmitting, i,e, $\mod\left(k, 2^{SF_n-7}\right) = 0$ and $\mod\left(j, 2^{SF_n-7}\right) = 0$. If user n is not transmitting but harvesting energy, the transmit power $p_n(j)$ is simply equal to zero watts. The causality conditions constraint at each user n at time slot k, having $\rho_n(k) = 1$, is that

$$0 \leq p_n(k) \leq P_t, \tag{15}$$

$$0 \leq p_n(k) \leq P_{A,n}(k), \tag{16}$$

which means that for a certain time slot k, each user n cannot use a power greater than the maximum transmit power and to the current available budget power in the previous time slots.

III. Packet Collision Time Between LoRa Users

In this section, we examine the general scenario of the packet collision time during time slot k between users using either the same or different SFs. Therefore, inter-SF interference between users using different SFs is also considered, namely the imperfect SF orthogonality case. We expect that the packet collision time is dependent on SF and the start time of the transmission. Let $col_{n,m}(k)$ be the collision time during the time slot k between the user n and the user m. At the time slot k, the users n and m are transmitting their $a_n(k)$-th and $a_m(k)$-th transmission attempts.

We consider the case where the users start transmitting immediately after finishing harvesting their energy. Meaning that the start time of transmission is exactly the same as the end of EH time. The total EH time duration per one transmission time is constrained to the off-time duration of the corresponding spreading factor. During the time slot k, the users n and m transmitting their $a_n(k)$-th and $a_m(k)$-th transmission attempts collide only at time slots k satisfying $\rho_n(k) = \rho_m(k) = 1$. Otherwise, the packet collision time is zero.

Theorem 1: When $\rho_n(k) = \rho_m(k) = 1$, the packet collision time between user n and user m depends on the total EH time per one transmission attempt, as well as the time on air. Its expression is given by (17) *and* (18)*, as shown at the bottom of the page, if $(\tau_{e,n}(k) - \tau_{e,m}(k))$ and $(T_{a,n} - T_{a,m})$ have the same sign, and by (18) if $(\tau_{e,n}(k) - \tau_{e,m}(k))$ and $(T_{a,n} - T_{a,m})$ have opposite signs.*

Proof: In order to derive the expression of the collision time between two users n and m, we consider two cases: either user n spends more time to harvest or less than user m. Firstly, if the user n requires more time to harvest than the user m at time slot k, i.e. $\tau_{e,n}(k) \geq \tau_{e,m}(k)$, the packet collision time depends on how much each user spends during the packet transmission as shown in Fig. 3. If the user m, that requires less time to harvest, finishes its packet transmission before the user n starts transmitting, then the two users will not collide. On the other hand, if the user m finishes its transmission after the user n finishes its own transmission, the two users will collide during the packet transmission time $T_{a,n}$ of the user n. Otherwise, if the user m finishes its transmission after the user n finished harvesting but before it finishes the transmission, the collision time will be $\tau_{e,m}(k) + T_{a,m} - \tau_{e,n}(k)$. Secondly, if the user n requires less time to harvest than the user m, i.e. $\tau_{e,n}(k) < \tau_{e,m}(k)$, the collision time is expressed by just exchanging the roles of the users n and m above. □

Remark 2: Note that the behaviour of the collision time in (17) *and* (18) *is independent of the EH time in two cases: 1) one user finishes harvesting and transmitting while the other user is still harvesting energy; 2) one user starts transmitting while the other user is still harvesting and the first user is still transmitting while the other user finishes transmitting.*

Corollary 1: The collision time depending on the EH time is always less or equal to the collision time in the worst case, which can be expressed as

$$col^{ws}_{n,m}(k) = \min\left(T_{a,m}, T_{a,n}\right). \tag{19}$$

This collision can happen when all users finish transmitting at the same time which is the worst interference case. In this case, the users with the lowest SF will undergo the lowest interference (highest rate per unit of time) and the users with the highest SF will undergo the highest interference (lowest rate per unit of time). However, the users with the lowest SF will have less time to transmit and harvest, while the users with the highest SF will have more time to transmit and subsequently harvest.

Corollary 2: If we consider the users using the same SF (i.e. $T_{a,n} = T_{a,m}$, $\forall m \neq n$), the collision time is only presented by (17)*. There is a collision between two users only if one of them starts transmitting while the other is transmitting and finishes his transmission before the first one. If we assign the same EH time to the users with the same SF, the collision time is always equal to the time on air.*

- If $(\tau_{e,n}(k) - \tau_{e,m}(k))$ and $(T_{a,n} - T_{a,m})$ have the same sign, then

$$col_{n,m}(k) = \begin{cases} 0, & \text{if } |\tau_{e,n}(k) - \tau_{e,m}(k)| \geq \min\left(T_{a,n}, T_{a,m}\right), \\ \min\left(T_{a,n}, T_{a,m}\right) - |\tau_{e,n}(k) - \tau_{e,m}(k)|, & \text{if } |\tau_{e,n}(k) - \tau_{e,m}(k)| < \min\left(T_{a,n}, T_{a,m}\right). \end{cases} \tag{17}$$

- If $(\tau_{e,n}(k) - \tau_{e,m}(k))$ and $(T_{a,n} - T_{a,m})$ have opposite signs, then

$$col_{n,m}(k) = \begin{cases} 0, & \text{if } |\tau_{e,n}(k) - \tau_{e,m}(k)| \geq \max\left(T_{a,n}, T_{a,m}\right), \\ \max\left(T_{a,n}, T_{a,m}\right) - |\tau_{e,n}(k) - \tau_{e,m}(k)|, & \text{if } |T_{a,m} - T_{a,n}| \leq |\tau_{e,n}(k) - \tau_{e,m}(k)| < \max\left(T_{a,n}, T_{a,m}\right), \\ \min\left(T_{a,n}, T_{a,m}\right), & \text{if } |\tau_{e,n}(k) - \tau_{e,m}(k)| < |T_{a,m} - T_{a,n}|. \end{cases} \tag{18}$$

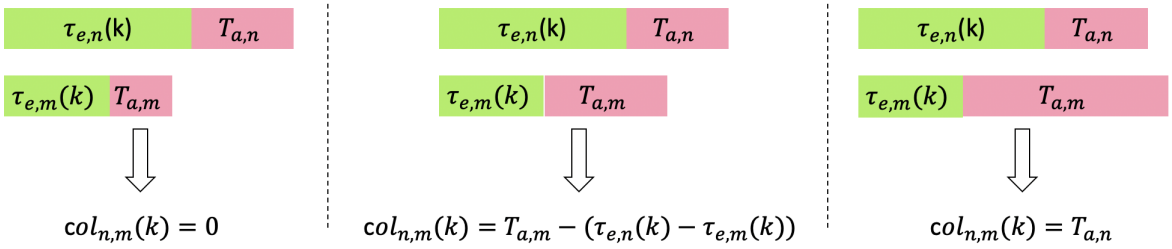

Fig. 3. Collision time depending on EH time for $\tau_{e,n}(k) > \tau_{e,m}(k)$ if two users start to transmit at the same time slot k.

Corollary 3: If all users are harvesting energy during their whole time-off durations, and we satisfy the condition $\frac{t_{a,i}}{t_{a,j}} > 1-d$, *for* $7 \leq j < i \leq 12$, *then users using different SFs do not collide during the odd time slots, even though the imperfect orthogonality exists between SFs.*

Proof: If the total EH time per one transmission attempt is equal to the off-time duration as $\frac{1-d}{d}T_{a,n}$, $\forall n$ and we satisfy the condition $\frac{t_{a,i}}{t_{a,j}} > 1-d$, for $7 \leq j < i \leq 12$, the collision time between the users simplifies to

$$col_{n,m}(k) = \begin{cases} 0, & \text{if } SF_n \neq SF_m, \\ T_{a,n}, & \text{if } SF_n = SF_m. \end{cases} \tag{20}$$

This expression means that, even though we have imperfect orthogonality between SFs, the users using different SFs do not collide over the time domain during the odd time slots. □

IV. Max-Min Throughput Optimization

Considering the packet collision time between users, the expression of signal-to-interference plus noise ratio (SINR) of the n-th user at time slot k is given by

$$\gamma_n^{col}(k) = \frac{p_n(k)g_n(k)}{\sum_{m \neq n} \rho_m(k)\mu_{n,m}(k)\ p_m(k)g_m(k) + \sigma^2}, \tag{21}$$

where σ^2 is the variance of the additive white Gaussian noise (AWGN) at the LoRa gateway, $\mu_{n,m}(k) = \frac{col_{n,m}(k)}{T_{a,m}}\xi_{n,m}$, and $\xi_{n,m}$ is the correlation factor between the coded waveforms for users m and n. Note that $\xi_{n,m} = 1$ if $m = n$ and $0 \leq \xi_{n,m} < 1$ if $m \neq n$. Moreover, for the users sharing the same SF over the same channel, the correlation factor will be much higher than that of users sharing different SFs. At the time slot $k = 1, \ldots, K$, the instantaneous transmission rate of user n corresponding to the $a_n(k)$-th transmission attempt is given by

$$R_n(k) = \rho_n(k)\log_2\left(1 + \gamma_n^{col}(k)\right), \tag{22}$$

only for n and m that are transmitting, i.e. $\rho_n(k) = \rho_m(k) = 1$. Subsequently, the temporal average of throughput rate of user n for the time period T can be written as

$$R_n = \frac{T_{a,n}}{T}\sum_{k=1}^{K} \rho_n(k)\log_2\left(1 + \gamma_n^{col}(k)\right). \tag{23}$$

Remark 3: Note that the SINR-based expression of the throughput rate suggests implicitly that LoRa has a certain immunity to interference in presence of packet time collision as long as the SINR is strong enough and the SNR values are above the receiver sensitivity. This fact is in agreement with recent results in [31] where it was shown that LoRa can work well even several users using the same SF when SIR is as low as 0dB.

In this paper, we aim to maximize the minimum of the temporal averaged uplink transmission rate of all LoRa users while optimizing the SF allocation, the EH time allocation, and the power allocation between users, which could be formulated as

$$\max_{T_{a,n}, \tau_{e,n}(k), p_n(k)} \min_{n \in U} \quad R_n = \frac{T_{a,n}}{T}\sum_{k=1}^{K} \rho_n(k) \times \log_2\left(1 + \gamma_n^{col}(k)\right), \tag{24a}$$

$$\text{s.t.} \quad \text{C}_1\text{: } 0 \leq p_n(k) \leq P_t, \tag{24b}$$

$$\text{C}_2\text{: } 0 \leq \sum_{j=1}^{k} \rho_n(k)p_n(j) \leq \sum_{j=1}^{k} \tau_{e,n}(j)\frac{E_n(j)}{T_{a,n}} \tag{24c}$$

$$\text{C}_3\text{: } 0 \leq \tau_{e,n}(k) \leq \tau_{e,n,max}(k) \tag{24d}$$

$$\text{C}_4\text{: } T_{a,n} \in \mathcal{T}_a. \tag{24e}$$

The constraint C_1 is due to the maximum transmit power constraint at each LoRa user. The constraint C_2 is because each user cannot transmit with a power greater than the available power. The constraint C_3 is due to the duty cycle restriction. The constraint C_4 is due to the different SF assignment at each user. This optimization problem is non-convex since it is a mixed-integer programming problem and the objective function is nonconcave due to the interference from colliding users. So, no computationally efficient method can be applied without involving exhaustive search, which has at least a complexity of the order of $U^{|\mathcal{T}_a|}N_\epsilon^2$, where N_ϵ is the complexity of the one-dimensional search method. To simplify the analysis, we propose to decouple the problem into three sub-problems where we optimize the three optimization variables separately. First, we assign the SF while respecting the LoRa specifications. Second, we optimize the EH time using the one-dimensional exhaustive search method. Finally, we optimize the transmit powers for the given SF and EH time.

A. Unfair and Fair SF Allocation Algorithms

First, we investigate the SF allocation between the LoRa users. In order to assign the SFs between the users, we need to satisfy some conditions from LoRa specifications.

The received signal at the gateway should exceed its sensitivity. The receiver sensitivity of the gateway depends on SF as shown in Table I in [8], [10]. In the literature, there are different ways to allocate the SFs between the users, as was mentioned in Section I. In [8], [10], the SFs are allocated according to the distance between the users and the gateway. In [17], the fair collision probability $P(SF = f) = \frac{f/2^f}{\sum_{i=7}^{12} i/2^i}$, for $f = 7, \ldots, 12$, has been proposed to avoid the near-far problems. In [18], the algorithm EXPLoRa-SF has been proposed to equally divide the SFs between the users while respecting the RSSI values and relevant constraints.

Aligned with all these schemes, we proceed as follows. First, respecting the specifications, we select the active users among all the users, whose RSSI values are above the minimum required receiver sensitivity at the gateway. Then, we proceed in two different ways that assure either fairness or unfairness between the users. The fair SF allocation makes use of the fair collision probability proposed in [17] to avoid the near-far problem. The unfair SF allocation is a simple scheme that equally divides the users to groups of equal sizes and ignores the fairness in terms of transmission time allocation.

First, we assume that all users transmit with the maximum power $P_{n,max}$ satisfying constraints C_1 and C_2, where $\tau_{e,n}(j)$ in the constraint C_2 is chosen equal to its maximum value $\tau_{e,n,max}(j)$ satisfying the constraint C_3 with equality. We compute the RSSIs of all users at the beginning of the first time slot. Respecting the specifications, we select the number U_a of active users that have an RSSI exceeding the minimum required sensitivity at the gateway $sensi_{min}$ corresponding to $SF = 12$ in Table 1 in [8]. We divide the U_a ordered users into $|S|$ groups of size k_f, $f = 1, \ldots, |S|$, according to the received power at the gateway. The size k_f, $f = 1, \ldots, |S|$ of each group is defined while assuring either fairness or unfairness between the users. The unfair SF allocation equally divides the users to $|S|$ groups of size $\frac{U_a}{|S|}$. The fair SF allocation uses the fair collision probability in [16]. More details are described in Algorithm 1.

Algorithm 1: Unfair/Fair SF Allocation Algorithms

Data: P_t, d, $E_n(k)$, U, $g_{n,1}$, $sensi_{min}$, S
Initialize $U_a = 0$;
for $n = 1 \rightarrow U$ **do**
  Compute $RSSI_n = P_{n,max} g_{n,1}$;
  if $RSSI_n \geq sensi_{min}$ **then** Increment U_a;
end
Order the U_a users s.t. $RSSI$s are in a descending way;
Divide the U_a ordered users into $|S|$ groups of size k_f, with $|S|$ being the number of available SFs;
for $f = 1 \rightarrow |S|$ **do**
  if *Unfair* **then** $k_f = \frac{U_a}{|S|}$ **else** $k_f = \frac{\frac{f+|S|}{2^{f+|S|}}}{\sum_{i=1}^{|S|} \frac{6+i}{2^{6+i}}} U_a$;
  for $n = \sum_{j=1}^{f-1} k_j + 1 \rightarrow \sum_{j=1}^{f} k_j$ **do** $SF_n = f + 6$;
end
return SF_n;

Complexity: If we do not respect the LoRa specifications, the optimal solution for the SF assignment between the users that maximizes the minimum rate involves an exhaustive search over a number of possibilities equal to $|S|^U$. The number of users U is usually very large. So, the exhaustive search for the SF allocation is computationally expensive and it is difficult to be performed due to software limitations. In order to reduce the complexity, we opt for the two low complex SF allocation algorithms explained in Algorithm 1 which both respect the LoRa specifications and align with what was done before in the literature.

B. EH Time Allocation

Since we are considering the HTT protocol, there is no data transmission during the energy harvesting period. Also, the optimal EH time $\tau_{e,n}(k)$ solution to (24) should satisfy the constraints C_2 and C_3. We propose to proceed successively where we optimize $\tau_{e,n}(k)$ given the values in the previous time slots. Let us denote by $\delta^{(1)}_{n,max}(k) = \tau_{e,n,max}(k)$ and $\delta^{(2)}_{n,max}(k) = \min\left(\frac{P_t T_{a,n}}{E_n(k)} a_n(k) - \sum_{j=1}^{k-1} \frac{\tau_{e,n}(j) E_n(j)}{E_n(k)}, \delta^{(1)}_{n,max}(k)\right)$.

Theorem 2: If the collision time in (17) *and* (18) *is a non monotonic function of the EH time, the optimal EH time* $\tau_{e,n}(k)$ *is obtained by a one-dimensional search method in the interval* $\left(0, \delta^{(1)}_{n,max}(k)\right]$. *If the collision time is a monotonic nonincreasing function of the EH time, the optimal EH time* $\tau_{e,n}(k)$ *is equal to* $\delta^{(1)}_{n,max}(k)$. *If the collision time is a monotonic nondecreasing function or independent of the EH time, the optimal EH time is equal to* $\delta^{(2)}_{n,max}(k)$.

Proof: Since we have a maximum transmit power constraint in C_1, we represent two possible cases: either we are harvesting more than what we need (i.e. $\sum_{j=1}^{k} \rho_n(j) P_t \leq \sum_{j=1}^{k} P_{h,n}(j)$) or we are harvesting less than what we need (i.e. $\sum_{j=1}^{k} \rho_n(j) P_t \geq \sum_{j=1}^{k} P_{h,n}(j)$).

If $\sum_{j=1}^{k} \rho_n(j) P_t \leq \sum_{j=1}^{k} P_{h,n}(j)$, the constraint C_2 is trivially satisfied and the EH time should satisfy

$$\delta^{(2)}_{n,max}(k) \leq \tau_{e,n}(k) \leq \delta^{(1)}_{n,max}(k). \tag{25}$$

At this point, one would say that it is wasteful harvesting more than what we need (i.e. $\sum_{j=1}^{k} \rho_n(j) P_t$). However, spending more time on harvesting may reduce/increase the collision time between users and hence increase/decrease the throughput rate. Since our interest is minimizing the collision, optimizing the EH time depends on the monotonicity of the collision time in function of the EH time. If the collision time is a non-monotonic function with respect to the EH time, the optimal EH time is obtained by a one-dimensional search method in $\left[\delta^{(2)}_{n,max}(k), \delta^{(1)}_{n,max}(k)\right]$, such as the bisection method [32]. If the collision time is a monotonic nonincreasing function with respect to the EH time, the optimal EH time is $\delta^{(1)}_{n,max}(k)$. If the collision time is a monotonic nondecreasing function with respect to the EH time (or independent of the EH time), the optimal EH time is $\delta^{(2)}_{n,max}(k)$. Otherwise, the optimal value is between $\delta^{(2)}_{n,max}(k)$ and $\delta^{(1)}_{n,max}(k)$. On the other hand, if $\sum_{j=1}^{k} \rho_n(j) P_t \leq \sum_{j=1}^{k} P_{h,n}(j)$, the EH time satisfies

$$0 < \tau_{e,n}(k) \leq \delta^{(2)}_{n,max}(k) \leq \delta^{(1)}_{n,max}(k). \tag{26}$$

Similarly, the EH time can be obtained by a one-dimensional search method and the optimal value of the EH time depends on the collision time. If the collision time is a nonincreasing function with respect to the EH time, the optimal EH time is $\delta^{(1)}_{n,max}(k)$, which is the maximum value. If the collision time is a nondecreasing function with respect to the EH time (or independent of the EH time), the optimal EH time is $\delta^{(2)}_{n,max}(k)$. ■

Corollary 4: If the collision time is given by the worst case scenario in (19)*, the optimal solution of the EH time $\tau_{e,n}(k)$ is exactly given by $\delta^{(2)}_{n,max}(k)$, which is proportional to $T_{a,n}$. The available power after harvesting at each LoRa user is independent of $T_{a,n}$. Thus, the preference of SF has no effect on the energy harvesting constraint at each LoRa.*

Proof: The proof is an immediate result of Theorem 1. ■

C. Transmit Power Optimization

Given the SF allocation and the EH time allocation, we then optimize the transmit powers $p_n(k)$s for all LoRa users.

1) Optimal Solution for Single Transmission: If all users have only one uplink transmission attempt, i.e. $a_{n,max} = 1$, $\forall n$, then they transmit at a single time slot denoted as k_n s.t. $\rho_n(k_n) = 1$ and $a_n(k_n) = 1$. The optimal transmit powers $p_n(k)$ for all LoRa users are solutions to

$$\max_{p_n(k_n)} \quad \min_{n\in U_a} \quad \log\left(1+\gamma_n^{col}(k_n)\right), \tag{27a}$$

$$\text{s.t.} \quad \text{C}_5\text{: } 0 \le p_n(k_n) \le \overline{P}_n = \min\left(P_t, \frac{\sum_{j=k_n-2^{SF_n-7}-1}^{k_n} \tau_{e,n}(j)}{T_{a,n}} E_n(j)\right). \tag{27b}$$

This problem is non-convex, therefore we introduce a new optimization variable t and have the following equivalent convex problem:

$$\max_{t,p_n(k_n),\forall n\in U_a} \quad t, \tag{28a}$$

$$\text{s.t.} \quad \text{C}_5\ ,\ \text{C}_6\text{: } t \le \log\left(1+\gamma_n^{col}(k_n)\right), \tag{28b}$$

$$\text{C}_7\text{: } t \ge 0 \tag{28c}$$

For a given $t_{low} \le t \le t_{up}$, the optimization problem is convex and the powers $p_n(k_n)$'s can be optimally obtained for a given t. Then, the optimal t can be selected using any one-dimensional search method such as the bisection search method [32].

2) Suboptimal Solution With CCCP for Multiple Transmissions: When $a_{n,max} > 1$, $\forall n$, we propose to use CCCP [33] which uses a first-order Taylor approximation to derive a concave lower bound on the objective function which transform the original optimization problem into an approximated convex problem. The procedure is as follows. First, we derive the lower bound on the instantaneous transmission rate of user n at time slot k at $p_n(k) = \hat{p}_n(k)$ as

$$R_n(k) = \log_2\left(1+\frac{p_n(k)\frac{g_n(k)}{\sigma^2}}{\sum_{m\neq n}\rho_m(k)\mu_{n,m}(k)p_m(k)\frac{g_m(k)}{\sigma^2}+1}\right) \tag{29}$$

$$= \log_2\left(\sum_m \rho_m(k)\mu_{n,m}(k)p_m(k)\frac{g_m(k)}{\sigma^2}+1\right) - \log_2\left(\sum_{m\neq n} \rho_m(k)\mu_{n,m}(k)p_m(k)\frac{g_m(k)}{\sigma^2}+1\right) \tag{30}$$

$$\ge R_{n,1}(k) + \hat{R}_{n,2}(k), \tag{31}$$

with

$$R_{n,1}(k) = \log_2\left(\sum_m \rho_m(k)\mu_{n,m}(k)p_m(k)\frac{g_m(k)}{\sigma^2}+1\right) - \frac{1+\sum_{m\neq n}\rho_m(k)\mu_{n,m}(k)p_m(k)\frac{g_m(k)}{\sigma^2}}{1+\sum_{m\neq n}\rho_m(k)\mu_{n,m}(k)\hat{p}_m(k)\frac{g_m(k)}{\sigma^2}}, \tag{32}$$

$$\hat{R}_{n,2}(k) = 1-\log_2\left(\sum_{m\neq n}\rho_m(k)\mu_{n,m}(k)\hat{p}_m(k)\frac{g_m(k)}{\sigma^2}+1\right). \tag{33}$$

Then, for a given $\hat{p}_n(k)$, for $\forall n = 1,\ldots,U$, $\forall k = 1,\ldots,K$, problem (24) simplifies to the equivalent optimisation problem as follows

$$\max_{p_n(k)} \min_{n\in U} \quad \hat{R}_n = \frac{T_{a,n}}{T}\sum_{k=1}^{K} R_{n,1}(k) + \frac{T_{a,n}}{T}\sum_{k=1}^{K}\hat{R}_{n,2}(k), \tag{34a}$$

$$\text{s.t.} \quad \text{C}_1\&\ \text{C}_2. \tag{34b}$$

This problem is still nonconvex. So, we introduce a new optimization variable t and we solve the following convex optimization problem

$$\max_{t,p_n(k)} \quad t, \tag{35a}$$

$$\text{s.t.} \quad \text{C}_1,\ \text{C}_2, \tag{35b}$$

$$\text{C}_8\text{: } t \le \frac{T_{a,n}}{T}\sum_{k=1}^{K} R_{n,1}(k) + \frac{T_{a,n}}{T}\sum_{k=1}^{K}\hat{R}_{n,2}(k),\ \forall n, \tag{35c}$$

$$\text{C}_9\text{: } 0 \le t \le t_{up}, \tag{35d}$$

where t_{up} is the maximum value that can be attained by t satisfying inequality C_6. The value of $\hat{p}_n(k)$ used in solving (35) is its solution in the previous iteration and it is initialized by a feasible point satisfying constraints C_1-C_2 and C_6-C_7. We summarise how Problem (35) is solved in Algorithm 2.

Algorithm 2: Power Allocation With CCCP

Data: U_a, Pt, ϵ, d, g_n, σ^2
At iteration $m = 0$, initialize $\hat{p}_n(k)^{m=0}$ by a feasible point satisfying C_1, C_2, C_8, and C_9;
while $\|p_n(k)^m - p_n(k)^{m-1}\| > \epsilon$ **do**
  Solve (35) for a given $\hat{p}_n(k)^{iter} = p_n(k)^{m-1}$;
  Increment m;
end
return $p_n(k)^m$;

V. Numerical Results

In this section, we present simulation results run in Matlab to validate our proposed solution.

A. LoRa Simulation Parameters

For LoRa network, the simulation parameters are chosen following the LoRa specifications [7]. The bandwidth is BW $=$ 125kHz, the duty cycle is 1%, and the SF ranges are from 7 to 12. The noise variance is defined as $\sigma^2 = -174 + \text{NF} + 10\log_{10}(\text{BW})$ in dBm, where NF is the noise figure equal to 6 dB. The number of symbols Nb_n for each user is defined as $Nb_n = n_{PR} + n_{PL,n} + 4.25$, where n_{PR} is the number of symbols in the preamble chosen equal to 12.25, $n_{PL,n}$ is the number of symbols in the payload equal to $8 + max\left(ceil\left(\frac{8\text{PL}-4SF_n+28+16}{4(SF_n-2\text{DE})}\right)(\text{CR}+4), 0\right)$, where the number of payload bytes is PL $=$ 10, the coding rate is CR $=$ 1, DE $=$ 1 for $SF \in \{11, 12\}$ and DE $=$ 0 for $SF \in \{7, \ldots, 10\}$. If the number of symbols is assumed to be the same for all SFs, we take $n_{PL,n} = 18$. The path-loss exponent for both the power transfer and the information transfer links is 3.5 for single transmission attempts and 3 for multiple transmission attempts. The radius R is taken equal to 100 meters. Unless specified, the maximum transmit power for all LoRa users is $P_t = 17$ dBm. In general, it is believed that the absolute maximum transmit power of low powered devices is 20 dBm. For LoRa, the maximum transmit power depends on the frequency, the locations, and the device class. For example, for 868 MHz, the maximum transmit power is 14 dBm in Europe. We chose 17 dBm as a value less than the maximum. and to challenge the EH nodes if they can harvest enough energy before transmitting.

B. RF Energy Harvesting Model

In our simulations, we are harvesting from the ambient RF signals transmitted by N_b power beacons (PBs) randomly located in the cell with radius R. The transmit power of PBs is P_b. An example of the network is presented in Fig. 4 where the power beacons density is 10^3 PBs/km^2 and the LoRa users density is 10^4 Users/km^2. Moreover, the harvested energy at each LoRa user depends on which EH model is considered either linear or nonlinear [26]. Unless specified, we use the nonlinear EH model [34] where a sigmoidal model was shown to fit the experimental data. For the sigmoidal model, if $P_{rec,n}$ is the received power from the PBs at the user n, the harvested energy E_n is expressed as

$$E_n = \Psi\left(P_{rec,n}\right), \tag{36}$$

where $\Psi(\cdot)$ is the function defined as $\Psi(x) = \frac{\beta(x)-M\Omega}{1-\Omega}$, $\beta(x) = \frac{M}{1+e^{-a(x-b)}}$, $\Omega = \frac{1}{1+e^{ab}}$, M is the maximum harvested energy, a and b are experimental parameters which reflect the nonlinear charging rate with respect to the input power and the minimum required turn-on voltage for the start of current flow through the diode, respectively. In all plotted figures, the nonlinear model is considered, with the parameters $a = 1500$, $b = 0.0022$, and $M = 24$ mW which were shown in [34] to fit the experimental data in [35]. Note that, if the linear model is considered, the harvested energy E_n is given by $E_n = \zeta P_{rec,n}$, where $\zeta \in [0, 1]$ is the conversion efficiency chosen equal to 0.6.

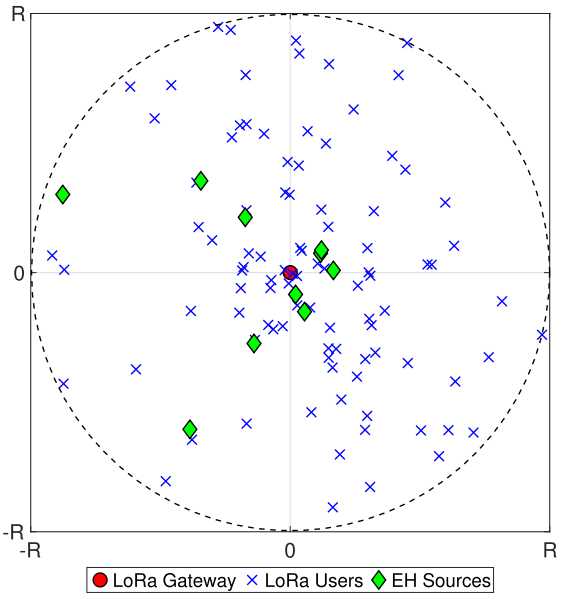

Fig. 4. An example of LoRa network consisted of one gateway and LoRa users with density 10^4 Users/km^2 harvesting from power beacons with density 10^3 PBs/km^2.

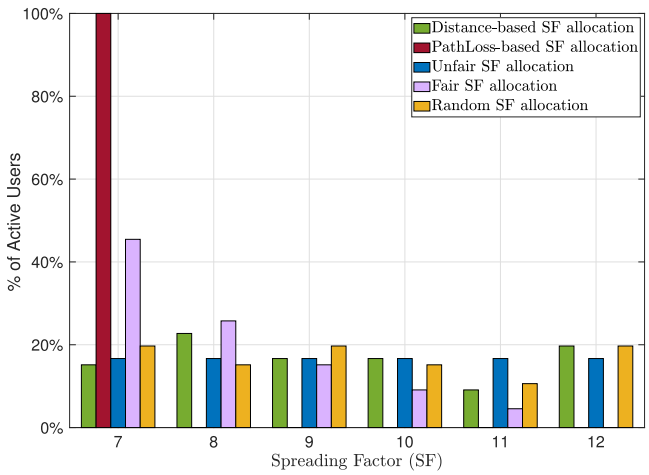

Fig. 5. Allocation of active users to different $SF \in \{7, \ldots, 12\}$ according to different allocation algorithms, for a density 10^4 Users/km^2.

C. One Uplink Transmission Attempt

First, we examine the case where all LoRa users intend to send only once, i.e. $a_{n,max} = 1, \forall n$. Here, the time slot index is omitted. The EH model used is the nonlinear EH model, with $P_b = 1$W, and $N_b = 10^3$ PBs/km^2.

1) Fairness vs Unfairness in SF Allocation Algorithms: In Fig. 5, we show the assignment of active users to different SFs, $SF \in \{7, \ldots, 12\}$, with different SF allocation algorithms. The fair and unfair SF allocation algorithms are the ones described in Algorithm 1. The distance-based SF allocation assigns the SFs depending on the distance between the users and the gateway [8]. Let $d_i = \frac{iR}{6}$, for $i = 0, \ldots, 6$.

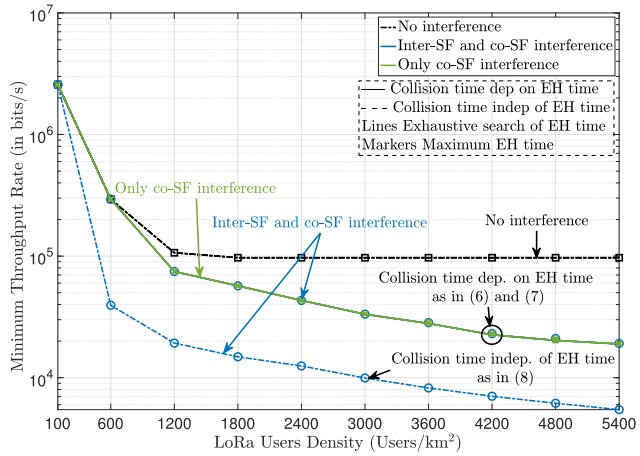

(a) Exhaustive search vs maximum EH time for unfair SF allocation.

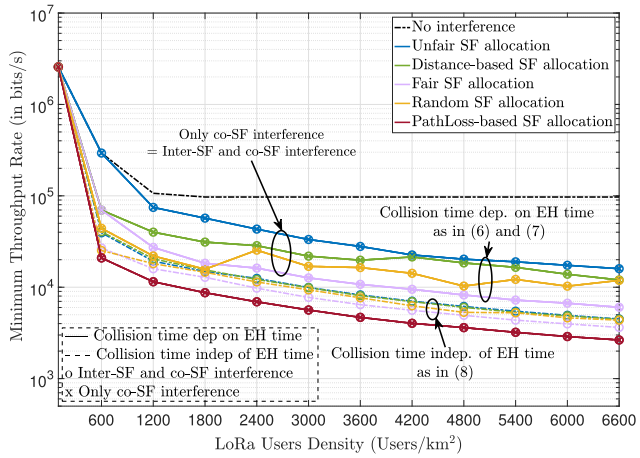

(b) Packet collision time either depending on EH time or not, with maximum EH time.

Fig. 6. Minimum throughput rate of LoRa users versus the density of active LoRa users per km^2, with optimal/maximum EH time and different SF allocation algorithms.

The users between the distances d_i and d_{i+1} will be assigned $SF = 7+i$, for $i = 0, \ldots, 5$. The pathloss-based SF allocation assigns the users while respecting Table I in [8], [10]. We can observe that the pathloss-based SF allocation, and the fair SF allocation tend to assign more users to lower SFs, while the other algorithms assign the users to all SFs. We will see in the following figures which one is better.

2) Optimal vs Maximum EH Time: In Fig. 6, we have plotted the minimum throughput rate of LoRa users versus the density of active LoRa users per km^2 with different SF allocation algorithms, and different multiuser interference scenarios (no interference, only co-SF interference, and inter-SF and co-SF interference). The no interference case refers to the case with correlation factor $\xi_{n,m} = 0$, $\forall n, m$. The only co-SF interference case refers to the case where the correlation factor $\xi_{n,m} = 1$ if the users n and m have the same SF and where the correlation factor $\xi_{n,m} = 0$ if the users n and m have different SFs. The inter-SF and co-SF interference case refers to the worst scenario case where $\xi_{n,m} = 1$, $\forall n, m$. The packet collision time is either depending on EH time as in (17) and (18); or not depending on EH time as in (19). Before comparing the SF allocation algorithms and the multiuser interference scenarios, we study first the choice of the EH time. In Fig. 6a, we have compared the results using the optimal EH time obtained using the exhaustive search and the maximum EH time, for the unfair SF allocation. The maximum value of EH time is equal to $T_{off,n}$ for the collision time depending on EH time; and equal to $\min\left(\frac{P_t}{E_n}, \frac{1-d}{d}\right) T_{a,n}$ for the collision time not depending on EH time in (19). The lined curves refer to the exhaustive search solution of EH time and the marked curves refer to the maximum value of EH time. In these plotted scenarios, we can see the agreement between the exhaustive search and the maximum value of EH time. Thus, in the following figures, we will consider the special case where the EH time is equal to its maximum value.

3) Collision Time and Multi-User Interference: In Fig. 6b, we have compared the results with the packet collision time depending on EH time (lines) and the ones with packet collision time not depending on EH time (dashed lines) for different SF allocation schemes. First of all, we can see that when the collision time is defined as in (17) and (18), the minimum rate outperforms the scenario where the collision time is defined in (19). This observation is expected since fewer users are transmitting simultaneously when the collision time depends on the EH time. Whereas, all users are transmitting simultaneously in (19). In addition, note that when $\tau_{e,n} = \delta^{(1)}_{n,max}$, the collision time simplifies to either zero if the users have different spreading factors, and to the time on air if the users have the same spreading factor, as shown in Corollary 3. This means that, for this case, the inter-SF interference does not exist. That is why we have an agreement between the minimum rate with the inter-SF and co-SF interference and the one with only co-SF interference, as shown in Fig. 6b. Hence, we can conclude that the expression of the collision time depending on the EH time protects the system from the inter-SF interference even though we consider imperfect orthogonality between the SFs. The remaining limitation of performance here is only due to the co-SF interference. Furthermore, the unfair SF allocation with the collision time expressed in (17) and $\tau_{e,n} = T_{off,n}$ reaches the nearest performance to the no interference case and outperforms the other SF allocation algorithms. The pathloss-based SF allocation has the poorest performance in terms of minimum rate. As shown in Fig. 5, this algorithm tends to assign more users to the lower SFs. Thus, we can conclude that the best performance is achieved while equally allocating the SFs between users and not while assigning the nearest users to the lowest SFs, in contrast with what was shown previously in [17].

4) Maximum Transmit Power: In Fig. 7a, we have plotted the proportion of active users having harvested an energy E_n greater or equal to $\frac{d}{1-d}P_t$, in which the active users are with density 2000 Users/km^2. This proportion plotted stands to the users transmitting with the maximum transmit power P_t. As the maximum transmit power increases, less users are capable of harvesting energy corresponding to the maximum transmit power. For a $P_t < -4$ dBm, the users are capable of harvesting energy greater or equal to P_t. For $P_t \geq -4$ dBm, we tend to have more energy scarcity as P_t increases. In Fig. 7b, we have plotted the corresponding

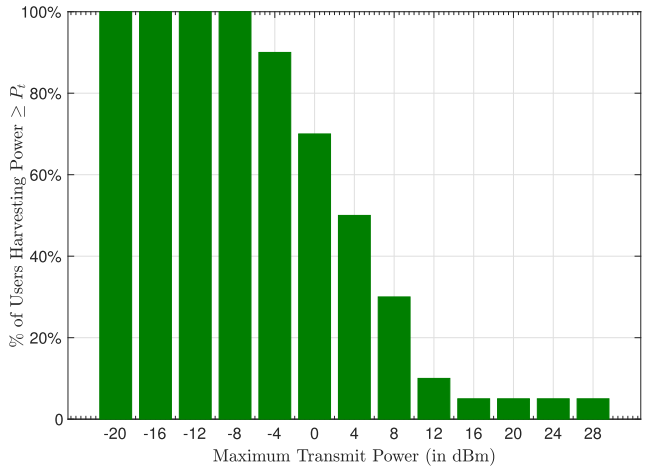

(a) % of active users having harvested enough energy.

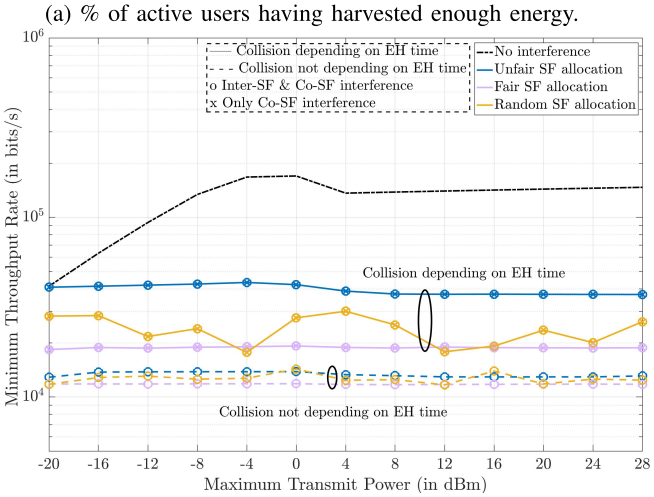

(b) Minimum throughput rate of LoRa users

Fig. 7. (a) The proportion of active users having harvested enough energy and (b) the minimum throughput rate of LoRa users versus maximum transmit power with density 2000 users per km^2.

minimum throughput rate of LoRa users versus the maximum transmit power for different SF allocation algorithms, different multiuser interference scenarios, and the packet collision time either depending or not on EH time. The active user density is the same as shown in Fig. 7a. The EH time is equal to its maximum value defined as previously. For $P_t < -4$ dBm, the minimum throughput rate of the different SF algorithms and multiuser interference cases tends to slowly increase compared to the no interference case. The slow motion in performance is limited by the co-SF interference. For higher transmit powers, the minimum throughput rate of all algorithms decreases slightly and saturates. Despite the energy scarcity shown in Fig. 7a, the minimum throughput rate did not decrease dramatically, as expected. This saturation behaviour is mainly governed by the co-SF interference limitation. Hence, we can conclude here that the co-SF interference is the main limitation of the throughput performance, not the energy scarcity.

D. Multiple Uplink Transmission Attempts

Next, we examine the case where LoRa users attempt to transmit data to the gateway multiple times, where maximum

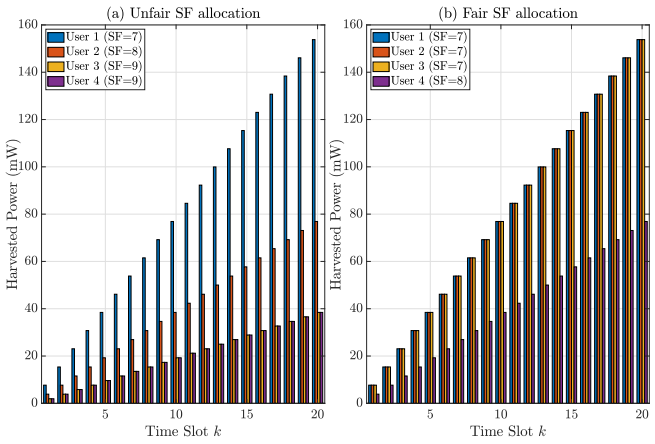

Fig. 8. Example of the total harvested power for 4 users for (a) unfair SF allocation and (b) fair SF allocation, with $K = 20$, and $SF \in \{7, 8, 9\}$.

number of attempts is defined by the SF assigned as in (10). Here, we choose $\rho_{2,n} = 1$, $\forall n$, which is the worst case scenario. In all the following plotted figures, we are comparing the fair and unfair SF allocation. We are also plotting the different multiuser interference scenarios: "no interference", "co-SF interference", and "co-SF & inter-SF interference". Also, the SFs are in $\in \{7, 8, 9\}$.

1) Number of Time Slots K: In Figs. 8, 9, and 10, we show the total harvested power for 4 exemplary users with $K = 20$, the transmit power and available power for 4 exemplary users for both $K = 4$ and $K = 16$, and the temporal average of the minimum data rate versus the number of time slots K, respectively, with the nonlinear EH model with $P_b = 0.1$W and $N_p = 10^4$ PBs/km^2.

In Fig. 8, it is observed that the total harvested power increases as the time slots increase for all users, as expected. Moreover, the users assigned to lower SFs are able to harvest more energy than higher SFs. We can see also that the user assigned to $SF = 7$ has harvested power greater than the maximum transmit power P_t from the time slot $k \geq 7$, for both fair and unfair SF allocations. The user assigned to $SF = 8$ has harvested power more than the maximum transmit power P_t from the time slot $k \geq 14$ for both fair and unfair SF allocations. The users assigned to $SF = 9$ for the unfair SF allocation have harvested power always less than the maximum transmit power P_t. At this point, it seems that users assigned to lower SFs tend to have more energy availability and suffer less from energy scarcity. Also, the fair SF allocation seems to have more users with less energy scarcity.

In Fig. 9, it is confirmed that users assigned to lower SFs are able to harvest more energy and they have more available power to use therefore. That means that the fair SF allocation scheme assures more energy available at the users than the unfair SF allocation scheme. That is because of more users assigned to lower SFs according to the fair SF allocation scheme. It induces that we have more simultaneous transmissions using the same SF, in addition to those using different SFs. Moreover, for $K = 4$, users are always harvesting less than P_t; whereas for $K = 16$, users with $SF = 7$ are harvesting energy close to P_t.

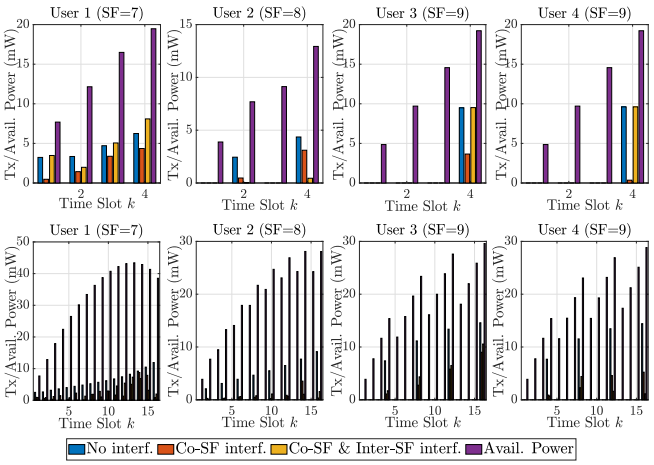

(a) Unfair SF allocation

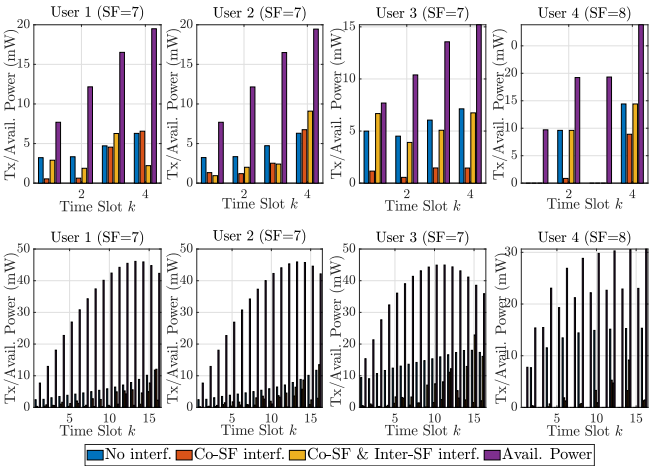

(b) Fair SF allocation

Fig. 9. Example of transmit power and available power for 4 users for (a) unfair SF allocation and (b) fair SF allocation, with $K = 4$ and $K = 16$.

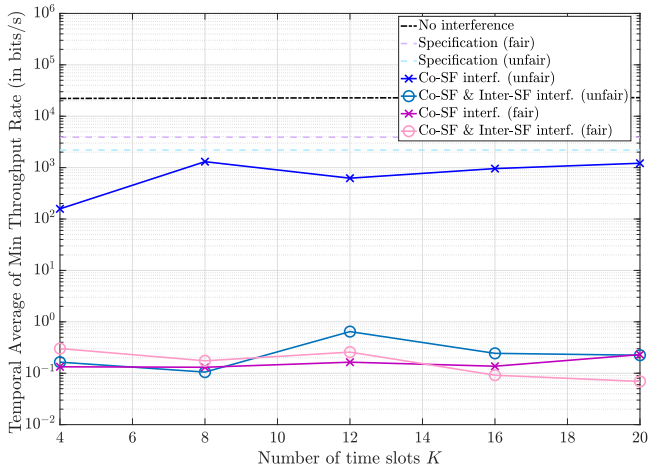

Fig. 10. Temporal average of minimum throughput rate vs number of time slots K, with $P_t = 17$dBm, $SF \in \{7, 8, 9\}$, and density 4 10^4 users/km^2.

In Fig. 10, we plot the temporal average of the minimum throughput rate versus the number of time slots K for unfair and fair SF allocation, with LoRa users density 410^4 per km^2. We also present the nominal rates claimed in the specifications, i.e. $R_n = \frac{SF_n}{2^{SF_n}} CR$ [6]. First, the performance of the temporal average of minimum rate with no interference is better than the one claimed in specifications; while the performance of the temporal average of minimum rate with interference is worse than the one claimed in specifications. In addition, we can see that the temporal average of minimum data rate is not significantly affected by the number of time slots K within a window T, which is an interesting result. Moreover, we see that the temporal average of minimum throughput rate with unfair SF allocation with only co-SF interference outperforms the one with fair SF allocation. It slightly increases as K increases. Also, the performance of unfair SF allocation is the closest performance to the one claimed by the specifications. However, when considering inter-SF interference, the temporal average of minimum throughput rate has a poor performance for both unfair and fair SF allocation schemes. This behaviour confirms the fact that the co-SF interference is the main limitation of the performance, not really the energy scarcity. In fact, we have seen in Figs. 8 and 9 that the fair SF allocation scheme assures more energy availability than the unfair SF allocation scheme. However, it encourages more users to transmit together with lower SFs. On the other hand, the unfair SF allocation assures that there is a moderate number of users assigned to each SF where a proportion of them may experience energy scarcity. To summarize results here, considering only co-SF interference and ignoring inter-SF interference, which stands for the case of perfect orthogonality between SFs, the unfair SF allocation outperforms the fair SF allocation because it induces less co-SF interference, even though it has more energy scarcity than the fair SF allocation.

2) Users Density: Fairness vs Unfairness: In Fig. 11, we have plotted the temporal average of minimum throughput rate versus the density of active LoRa users. The nonlinear EH model is considered with $P_b = 1$W and $N_p = 10^3$ PBs/km^2. We have plotted also the nominal rate in specifications [6]. In Fig. 11a, all users are assigned to $SF = 7$, and hence all SF allocation schemes perform alike. We have verified that we have the same performance for both $K = 1$ and $K = 4$ in Fig. 11a. In Fig. 11b, the users are assigned to SFs in $\{7, 8, 9\}$, and we examine the different SF allocation algorithms: distance-based SF allocation, unfair SF allocation, and fair SF allocation. First, in Figs. 11a and 11b the same observation regarding the nominal rate in specifications as in Fig. 10 where the performance of the temporal average of minimum rate is higher than the nominal rate in the specification for no interference case and lower than the nominal rate in the specification for the interference case. The co-SF interference case is below the specifications case for users density above 5000 per km^2. Moreover, for $K = 4$, the unfair SF allocation is outperforming both the fair SF allocation and distance-based SF allocation, with only co-SF interference. When considering inter-SF interference, the performance of all SF allocation schemes drop similarly. The case having only co-SF interference achieves better performance, which stands for the case of perfect orthogonality between SFs.

3) Maximum Transmit Power: Linear vs Nonlinear EH Model: In Figs. 12, 13, and 14, we present the instantaneous transmit power for 3 exemplary users with $K = 4$ and two

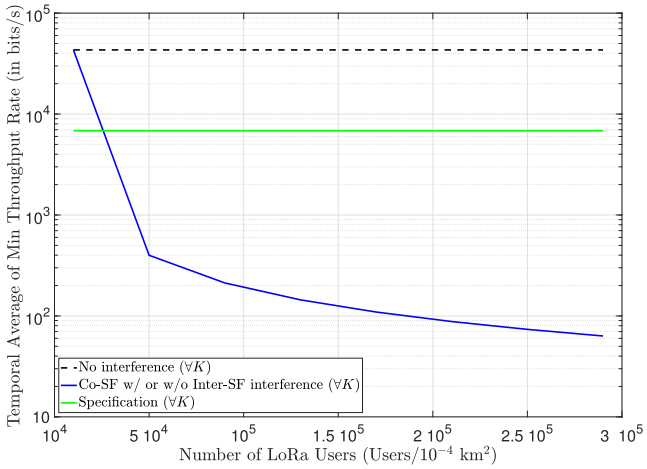

(a) K = 1&4, and $SF \in \mathcal{S} = \{7\}$

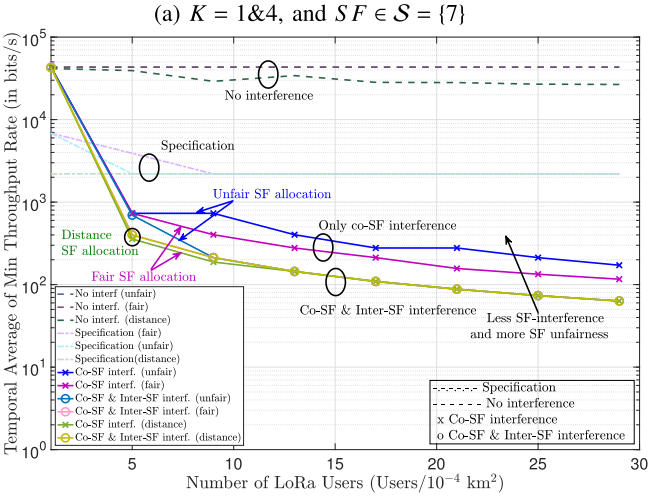

(b) K = 4, and $SF \in \mathcal{S} = \{7, 8, 9\}$

Fig. 11. Temporal average of minimum data rate vs LoRa users density per km^2 for different SF allocation algorithms, and different interference scenarios, with $P_t = 17$dBm.

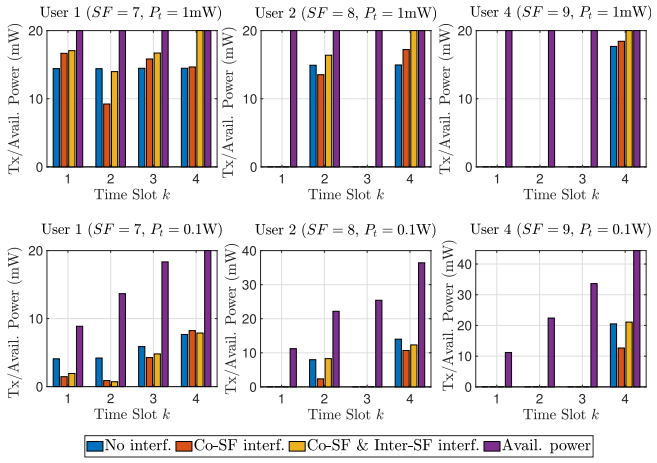

(a) Unfair SF Allocation

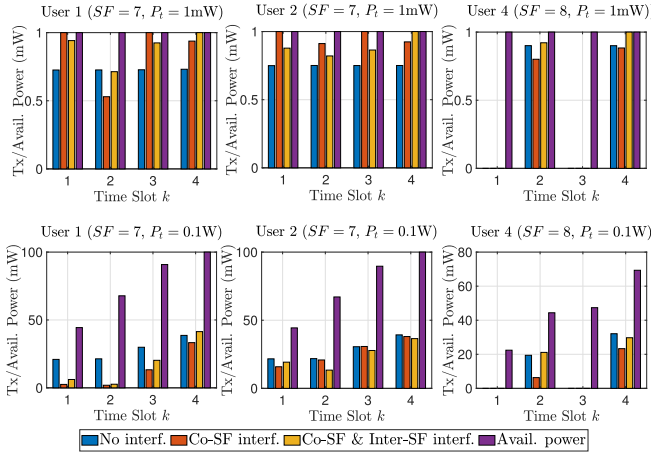

(b) Fair SF allocation

Fig. 12. Example of transmit/available powers for 4 exemplary users for unfair/fair SF allocation schemes, nonlinear EH model, with $P_t = 1$mW (top subfigures) and $P_t = 0.1$W (bottom subfigures), and $K = 4$.

different maximum transmit powers ($P_t = 1$mW and $P_t = 0.1$W), the total harvested power for 10 exemplary users with $K = 4$, and the temporal average of the minimum throughput rate versus the maximum transmit power P_t in dBm. The linear and nonlinear EH models are considered with $P_b = 1$W and $N_p = 10^3$ PBs/km^2.

In Fig. 13, we can see that the assignment of the users is independent of the linearity of the EH model. The users are assigned to the same SFs for both the linear and nonlinear EH models. In addition, considering the nonlinear EH model, the users are able to harvest more energy. Particularly, the maximum harvested power for the linear EH model is 0.12 W, while it is 0.18W for the nonlinear EH model.

In Fig. 12, the nonlinear EH model and two different maximum transmit powers ($P_t = 1$mW (top three ones) and $P_t = 0.1$W (bottom three ones)) are considered. Three exemplary users are considered in Fig. 12 whose SF assignment depends on the SF allocation algorithm considered. They are assigned to SFs $(7, 8, 9)$ in Fig. 12a; while they are assigned to SFs $(7, 7, 8)$ in Fig. 12b, respectively. First, increasing the maximum transmit power from $P_t = 1$mW to $P_t = 0.1$W, decreases the instantaneous powers of

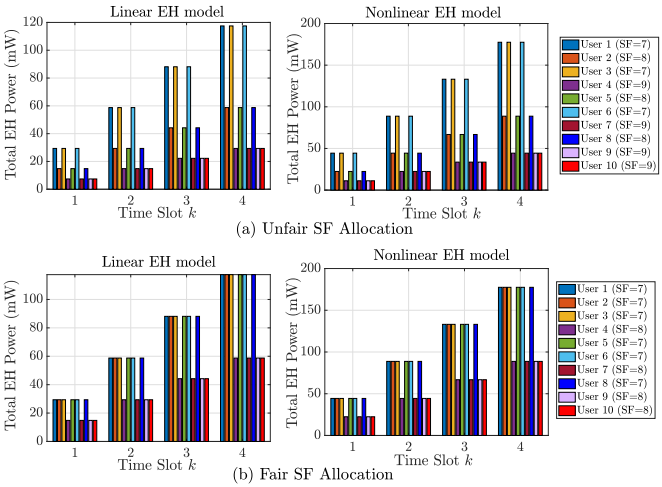

Fig. 13. Example of the total harvested power for 10 exemplary users with $K = 4$.

the three users considered here for both fair and unfair SF allocation algorithms. Moreover, when $P_t = 1$mW, the available powers for the three users for both fair and unfair SF allocation schemes are equal to P_t. No energy scarcity occurs

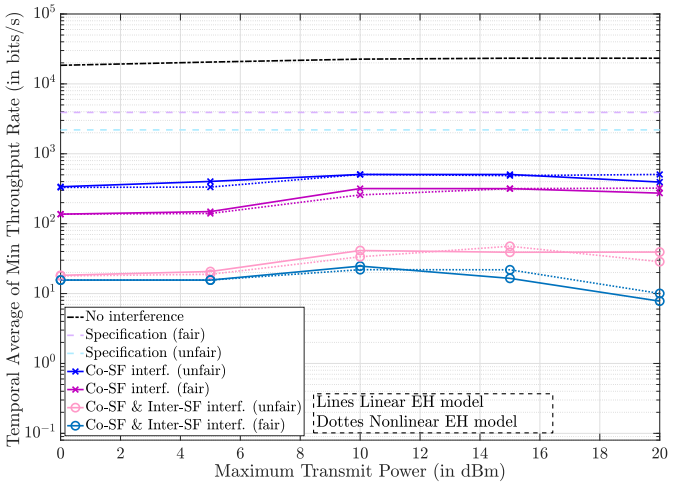

Fig. 14. Temporal average of minimum data rate vs P_t in dBm with $K = 4$, and $SF \in \{7, 8, 9\}$.

in this case. However, when the maximum transmit power becomes $P_t = 0.1$W, the users are in energy scarcity for the three first time slots. User 1 assigned to $SF = 7$ in both Figs. 12a and 12b has available power equal to the maximum transmit power at time slot $k = 4$. Also, user 2 in Fig. 12b has available power equal to the maximum transmit power at time slot $k = 4$ for the fair SF allocation scheme.

In Fig. 14, the maximum transmit power P_t ranges from 0 dBm to 20 dBm, which is wider than what LoRa devices are actually using. Usually, the maximum transmit power at LoRa devices are between 14 dBm and 17 dBm in practice. First, we can see that there is no much impact of the linearity and nonlinearity of the EH model on the temporal average of the minimum throughput rate. The temporal average of the minimum throughput rate with unfair SF allocation algorithm is always outperforming the one with fair SF allocation algorithm, with co-SF interference only. Moreover, the temporal average of minimum throughput rate is not highly affected by P_t even though we experience energy scarcity in some cases, which confirms our conclusion in the case of single transmission attempt that the co-SF interference is the main limitation of system performance rather than energy scarcity.

VI. Conclusion

In this paper, we have studied the uplink resource allocation in LoRa networks powered by ambient EH sources with imperfect SF orthogonality. First, the packet collision time between users using different SFs was expressed in function of the EH time duration. We have proposed SF allocation algorithms, which emphasise either fairness or unfairness between the users. We optimized the power allocation either optimally for single transmission attempt or suboptimally using CCCP procedure for multiple transmission attempts. Through the simulation results, we have seen that using the unfair SF allocation outperforms all the other scenarios while properly expressing the collision time between users in function of the EH time. This calls out to proper transmission scheduling in LoRa networks. Also, we have seen that co-SF interference is the main limitation to throughput performance and not energy scarcity. This result underlines the need to consider interference management techniques in LoRa networks.

References

[1] F. Benkhelifa, Z. Qin, and J. McCann, "Minimum throughput maximization in LoRa networks powered by ambient energy harvesting," in *Proc. IEEE Int. Conf. Commun. (ICC)*, Shanghai, China, May 2019, pp. 1–7.

[2] A. Al-Fuqaha, M. Guizani, M. Mohammadi, M. Aledhari, and M. Ayyash, "Internet of Things: A survey on enabling technologies, protocols, and applications," *IEEE Commun. Surveys Tuts.*, vol. 17, no. 4, pp. 2347–2376, 4th Quart., 2015.

[3] U. Raza, P. Kulkarni, and M. Sooriyabandara, "Low power wide area networks: An overview," *IEEE Commun. Surveys Tuts.*, vol. 19, no. 2, pp. 855–873, 2nd Quart., 2017.

[4] *Sigfox*. Accessed: Oct. 1, 2018. [Online]. Available: https://www.sigfox.com

[5] Y.-P.-E. Wang *et al.*, "A primer on 3GPP narrowband Internet of Things," *IEEE Commun. Mag.*, vol. 55, no. 3, pp. 117–123, Mar. 2017.

[6] S. Corporation. *LoRa Modulation Basics—AN1200.22, Revision 2*. Accessed: Oct. 1, 2018. [Online]. Available: https://www.semtech.com/uploads/documents/an1200.22.pdf

[7] J. Petäjäjärvi, K. Mikhaylov, M. Pettissalo, J. Janhunen, and J. Iinatti, "Performance of a low-power wide-area network based on LoRa technology: Doppler robustness, scalability, and coverage," *Int. J. Distrib. Sensor Netw.*, vol. 13, no. 3, 2017, Art. no. 1550147717699412.

[8] O. Georgiou and U. Raza, "Low power wide area network analysis: Can LoRa scale?" *IEEE Wireless Commun. Lett.*, vol. 6, no. 2, pp. 162–165, Apr. 2017.

[9] Z. Qin, Y. Liu, G. Y. Li, and J. A. McCann, "Performance analysis of clustered LoRa networks," *IEEE Trans. Veh. Technol.*, vol. 68, no. 8, pp. 7616–7629, Aug. 2019.

[10] J.-T. Lim and Y. Han, "Spreading factor allocation for massive connectivity in LoRa systems," *IEEE Commun. Lett.*, vol. 22, no. 4, pp. 800–803, Apr. 2018.

[11] Z. Qin and J. A. McCann, "Resource efficiency in low-power wide-area networks for IoT applications," in *Proc. IEEE Global Commun. Conf. (GLOBECOM)*, Dec. 2017, pp. 1–7.

[12] A. Waret, M. Kaneko, A. Guitton, and N. El Rachkidy, "LoRa throughput analysis with imperfect spreading factor orthogonality," *IEEE Wireless Commun. Lett.*, vol. 8, no. 2, pp. 408–411, Apr. 2019.

[13] A. Mahmood, E. Sisinni, L. Guntupalli, R. Rondon, S. A. Hassan, and M. Gidlund, "Scalability analysis of a LoRa network under imperfect orthogonality," *IEEE Trans. Ind. Informat.*, vol. 15, no. 3, pp. 1425–1436, Mar. 2019.

[14] K. Li, F. Benkhelifa, and J. McCann, "Resource allocation for non-orthogonal multiple access (NOMA) enabled LPWA networks," in *Proc. IEEE Global Commun. Conf. (GLOBECOM)*, Dec. 2019, pp. 1–6.

[15] Y.-K. Kim and S.-Y. Kim, "Success probability characterization of long-range in low-power wide area networks," *Sensors*, vol. 20, no. 23, p. 6861, Nov. 2020. [Online]. Available: https://www.mdpi.com/1424-8220/20/23/6861

[16] B. Reynders, W. Meert, and S. Pollin, "Power and spreading factor control in low power wide area networks," in *Proc. IEEE Int. Conf. Commun. (ICC)*, May 2017, pp. 1–6.

[17] K. Q. Abdelfadeel, V. Cionca, and D. Pesch, "Fair adaptive data rate allocation and power control in LoRaWAN," in *Proc. IEEE 19th Int. Symp. World Wireless, Mobile Multimedia Netw. (WoWMoM)*, Jun. 2018, pp. 14–15.

[18] F. Cuomo, M. Campo, A. Caponi, G. Bianchi, G. Rossini, and P. Pisani, "EXPLoRa: Extending the performance of LoRa by suitable spreading factor allocations," in *Proc. IEEE 13th Int. Conf. Wireless Mobile Comput., Netw. Commun. (WiMob)*, Oct. 2017, pp. 1–8.

[19] L. Amichi, M. Kaneko, E. H. Fukuda, N. El Rachkidy, and A. Guitton, "Joint allocation strategies of power and spreading factors with imperfect orthogonality in LoRa networks," *IEEE Trans. Commun.*, vol. 68, no. 6, pp. 3750–3765, Jun. 2020.

[20] C. Caillouet, M. Heusse, and F. Rousseau, "Optimal SF allocation in LoRaWAN considering physical capture and imperfect orthogonality," in *Proc. IEEE Global Commun. Conf. (GLOBECOM)*, Waikoloa, HI, USA, Dec. 2019, pp. 1–6.

[21] M. A. Ullah, J. Iqbal, A. Hoeller, R. Souza, and H. Alves, "K-means spreading factor allocation for large-scale LoRa networks," *Sensors*, vol. 19, no. 21, p. 4723, Oct. 2019.

[22] S. Kim, H. Lee, and S. Jeon, "An adaptive spreading factor selection scheme for a single channel LoRa modem," *Sensors*, vol. 20, no. 4, p. 1008, Feb. 2020.

[23] *Battery Market for IoT by Type, Rechargeability, End-Use Application and Geography—Global Forecast to 2025*. Accessed: Dec. 1, 2020. [Online]. Available: https://www.reportlinker.com
[24] M. Costa, T. Farrell, and L. Doyle, "On energy efficiency and lifetime in low power wide area network for the Internet of Things," in *Proc. IEEE Conf. Standards Commun. Netw. (CSCN)*, Sep. 2017, pp. 258–263.
[25] B. Su, Z. Qin, and Q. Ni, "Energy efficient uplink transmissions in LoRa networks," *IEEE Trans. Commun.*, vol. 68, no. 8, pp. 4960–4972, Aug. 2020.
[26] B. Clerckx, R. Zhang, R. Schober, D. W. K. Ng, D. I. Kim, and H. V. Poor, "Fundamentals of wireless information and power transfer: From RF energy harvester models to signal and system designs," *IEEE J. Sel. Areas Commun.*, vol. 37, no. 1, pp. 4–33, Jan. 2019.
[27] F. Orfei, C. B. Mezzetti, and F. Cottone, "Vibrations powered LoRa sensor: An electromechanical energy harvester working on a real bridge," in *Proc. IEEE SENSORS*, Oct. 2016, pp. 1–3.
[28] W.-K. Lee, M. J. W. Schubert, B.-Y. Ooi, and S. J.-Q. Ho, "Multi-source energy harvesting and storage for floating wireless sensor network nodes with long range communication capability," *IEEE Trans. Ind. Appl.*, vol. 54, no. 3, pp. 2606–2615, May 2018.
[29] M. Magno, F. A. Aoudia, M. Gautier, O. Berder, and L. Benini, "WULoRa: An energy efficient IoT end-node for energy harvesting and heterogeneous communication," in *Proc. Design, Autom. Test Eur. Conf. Exhib. (DATE)*, Mar. 2017, pp. 1528–1533.
[30] A. Kansal, J. Hsu, S. Zahedi, and M. B. Srivastava, "Power management in energy harvesting sensor networks," *ACM Trans. Embedded Comput. Syst.*, vol. 6, no. 4, p. 32, Sep. 2007. [Online]. Available: https://www.microsoft.com/en-us/research/publication/power-management-in-energy-harvesting-sensor-networks/
[31] L. Beltramelli, A. Mahmood, P. Osterberg, and M. Gidlund, "LoRa beyond ALOHA: An investigation of alternative random access protocols," *IEEE Trans. Ind. Informat.*, vol. 17, no. 5, pp. 3544–3554, May 2021.
[32] M. Grant and S. Boyd. (Mar. 2014). *CVX: MATLAB Software for Disciplined Convex Programming, Version 2.1*. [Online]. Available: http://cvxr.com/cvx
[33] A. L. Yuille and A. Rangarajan, "The concave-convex procedure," *Neural Comput.*, vol. 15, no. 4, pp. 915–936, Apr. 2003, doi: 10.1162/08997660360581958.
[34] E. Boshkovska, D. W. K. Ng, N. Zlatanov, and R. Schober, "Practical non-linear energy harvesting model and resource allocation for SWIPT systems," *IEEE Commun. Lett.*, vol. 19, no. 12, pp. 2082–2085, Dec. 2015.
[35] J. Guo and X. Zhu, "An improved analytical model for RF-DC conversion efficiency in microwave rectifiers," in *IEEE MTT-S Int. Microw. Symp. Dig.*, Jun. 2012, pp. 1–3.

Fatma Benkhelifa (Member, IEEE) was born in Tunis, Tunisia. She received the Diplôme d'Ingénieur degree from the École Polytechnique de Tunis (EPT), La Marsa, Tunisia, in 2011, and the M.Sc. and Ph.D. degrees in electrical engineering from the King Abdullah University of Science and Technology (KAUST), in 2013 and 2017, respectively.

Since January 2018, she joined Imperial College London, where she is currently a Research Associate with the Adaptive Embedded Systems Engineering (AESE) Research Group, Computing Department. Her research interests include energy harvesting, simultaneous wireless information and power transfer, stochastic geometry and queueing theory, LoRa networks, cooperative communications, cognitive radio networks, multi-user detection, interference management, low-SNR characterization, and energy-efficient wireless communications. She is an Editor Lead of "Low Power Wide area networks (LPWAN) and Long Range (LoRa) networks?" and Review editor in *Frontiers in Communications and Networks*, as well as a TPC Member in various conferences and journals.

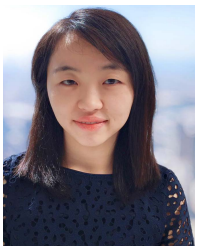

Zhijin Qin (Member, IEEE) received the B.S. degree from the Beijing University of Posts and Telecommunications, Beijing, China, in 2012, and the Ph.D. degree in electronic engineering from the Queen Mary University of London (QMUL), London, U.K., in 2016. She was a Post-Doctoral Research Associate with Imperial College London, from 2016 to 2017 and then a Lecturer with Lancaster University, from 2017 to 2018. Since 2018, she has been a Lecturer with the School of Electronic Engineering and Computer Science, QMUL. Her research interests include semantic communications, compressive sensing, and intelligent resource management in IoT applications. She was a recipient of the 2017 IEEE GLOBECOM Best Paper Award and the 2018 IEEE Signal Processing Society Young Author Best Paper Award. She serves as an Associate Editor for IEEE TRANSACTIONS ON COMMUNICATIONS, IEEE COMMUNICATIONS LETTERS, and IEEE TRANSACTIONS ON COGNITIVE COMMUNICATIONS AND NETWORKING.

Julie A. McCann (Member, IEEE) is currently a Professor in computer systems with Imperial College London. Her research interests include decentralized and self-organizing scalable algorithms and protocols for spatial computing e.g., wireless sensor systems, the Internet of Things, or CYBER-physical systems. She also leads the Adaptive Embedded Systems Engineering Research (AESE) Research Group, the Co-Director of the PeTraS the U.K., National Centre of Excellence for IoT Cybersecurity, is the PI in substantive international research collaborations with China (Digital Oceans), with Singapore (Eco-Cities), and co-directed the Intel Collaborative Research Institute for Sustainable Cities. She has received significant funding through national and international bodies, such as the U.K.,s Engineering and Physical Sciences Research Council (EPSRC), North American Electric Reliability Corporation, EU FP7/H2020 funding and Singapore NRF; she has a sub-lab in Singapore with I2R and HDB. She is an Elected Peer of the EPSRC. She serves on/chairs international conference committees, is a fellow of the BCS and Chartered Engineer, AESE was awarded the President's Medal for Research Excellence in 2020.